International Business Research; Vol. 5, No. 9; 2012
ISSN 1913-9004 E-ISSN 1913-9012
Published by Canadian Center of Science and Education

Short-term Dependence in Time Series as an Index of Complexity: Example from the S&P-500 Index

C-René Dominique[1] & Luis Eduardo Rivera Solis[2]

[1] Formerly Titular Professor of Applied Economics, Laval University, Quebec, Canada

[2] Professor of Finance, Townsend School of Business, Dowling College, New York, United States

Correspondence: Luis Eduardo Rivera Solis, Professor of Finance, Townsend School of Business, Dowling College, Oakdale, New York 11769, United States. E-mail: riveral@dowling.edu

Received: June 22, 2012 Accepted: July 25, 2012 Online Published: August 8, 2012

doi:10.5539/ibr.v5n9p38 URL: http://dx.doi.org/10.5539/ibr.v5n9p38

Abstract

The capital market is a reflexive dynamical input/output construct whose output (time series) is usually assessed by an index of roughness known as Hurst's exponent (H). Oddly enough, H has no theoretical foundation, but recently it has been found experimentally to vary from persistence (H > 1/2) or long-term dependence to anti-persistence (H < 1/2) or short-term dependence. This paper uses the thrown-offs of quadratic maps (modeled asymptotically) and singularity spectra of fractal sets to characterize H, the alternateness of dependence, and market crashes while proposing a simpler method of computing the correlation dimension than the Grassberger-Procaccia procedure.

Keywords: Hurst Exponent, anti-persistence, fractal attractors, SDIC, chaos, inherent noise, market crashes, Renyi's generalized fractal dimensions

1. Introduction

In response to the failure of the ordinary Brownian motion to characterize time series in economics and finance, Mandelbrot and van Ness (1968) introduced the stochastic motion known as the fractional Brownian motion (fBm). It is a special centered Gaussian field with stationary increments, vanishing at zero, indexed and characterized by the Hurst's (1951) exponent, H ε (0, 1). In financial economics, H > 1/2 is taken to be an indicator of long-term dependence or persistence in time series, i. e., the relative tendency of the time series to cluster in a given direction, while H < 1/2 is associated with short-term dependence, i. e., to regress to the mean. To account for changes in dependence, this analysis will posit Z_t as the observed *output* of the stochastic process, the fBm's as the *inputs* and the *r*'s as parameters characterizing changes in inputs (see Section 2.4).

The Hurst exponent can only be determined experimentally because it has no theoretical foundation. However, in most cases, its computed values vary inexplicably with series' lengths, with sampling intervals, and over time (Cutland, *et al*., 1993; Kaplan & Jay Kuo, 1993; Greene & Fielitz, 1997; Alvarez-Ramirez, *et al*., 2008). This in itself is baffling enough, but as a consequence nonetheless, after close to 50 years of application, the question as to whether financial time series are persistent, anti-persistent or both cannot elicit a conclusive answer.

There have been some advances in recent times, however. Chief among them is the introduction of the so-called Mixed fractional Brownian motion (MfBm) (Zili, 2006; Thale, 2009; Dominique & Rivera, 2011, among others). Dominique and Rivera have used an MfBm (see definition in Section 2.4) to show that the S&P-500 Index, for example, is persistent over some segments and anti-persistent over others. But the reason for this alternateness is in need of reinforcement. To that effect, we are proposing a very efficient and simple approach which consists of linking the index to other modern concepts such as the geometry of 'strange' attractors, and the multifractal formalism.

This paper will first show that indeed the H index is intricately linked to both the geometry and the dynamics of strange attractors as made constructive in quadratic maps. And it also recalls that the goal of multifractal analysis is to study the dimensional properties of the level sets of non-uniform and non-homogenous systems using either the Hausdorff dimension or topological entropy in the sense of Bowen; there, the H index, or equivalently the Hausdorff dimension (H), plays an important role in characterizing the singularity spectrum of time series. Then the paper will next use the clues thrown-off by the analysis of attractors and the features of singularity spectra to

establish the H index as a reliable index of complexity, de-fanging thus the notion of anti-persistence as well as the cause of the alternateness of persistence and anti-persistence.

2. The Index as a Discreet Characteristic of Strange Attractors

There is ample evidence that the evolution of both economic and financial time series is governed by strange attractors (Invernizzi & Medio, 1991; Medio, 1992; Peters, 1991), but strangely enough, most studies of time series in these disciplines seem to omit that essential connection. This section will attempt to mitigate that omission. But for tractability and completeness, we first review a few basic concepts.

2.1 The Characteristics of Strange Attractors

Let: **g**: E $\rightarrow$ E be a diffeomorphism of a smooth Riemanian manifold E $\subset \Re^n$; let ϕ_t (.) be the flow, and U (B) be a neighborhood of B $\subset$ E. If ϕ_t (.) $\subset$ U (B) at time t $\geq$ 0 and ϕ_t (.) $\rightarrow$ B as t$\rightarrow \infty$, then B is a compact hyperbolic attractor for **g**. Bowen has shown that the evolution of the Lebesque measure in U (B) converges to the Bowen-Ruelle-Sinai measure as it describes the orbit distribution of points in U (B), which are typical with respect to the Lebesque measure. The distribution is not uniform, however. There exist zero volume regions of high and low densities of visits by different orbits. This is made explicit immediately below.

B is a *strange* invariant set if it contains a countable subset of periodic orbits of large periods (denoted Γ_p), an uncountable subset of non-periodic orbits (Γ_{np}), and a dense orbit (Γ_d). To simplify, these orbits are next labeled "stable", "unstable", and "dense". Furthermore, these orbits reside in B which consists of a multitude of branched and interleaved surfaces or subsets that do intersect. Trajectories (Γ), on the other hand, do not intersect, but may move from one branched subset to another as they circulate.

Stable orbits are tangent to the direction of contraction. Unstable orbits are tangent to the direction of stretching. And a dense orbit is defined as:

Definition 1: If C is a subset of B, C is said to be dense in B if for every point b ε B and a $\delta > 0$, there is a point c ε C such that /b - c/ < δ.;

And:

Definition 2: In the Eckmann-Ruelle' (1985) sense, if any two points y_1, y_2 ε U (B) at t $\geq$ 0 becomes exponentially distant as t $\rightarrow \infty$, then sensitive dependence on initial conditions (SDIC) exists.

Thus, the presence of Γ_s, Γ_u, establishes that B is a hyperbolic invariant set; the presence of Γ_s, Γ_u and Γ_d establishes that B is *strange*. If additionally there is SDIC, then B is *chaotic*. Moreover, due to the loss of energy, the volume of U (B) shrinks, turning B into a multifaceted "thin" set that comprises all these interleaved subsets of points of zero volume (reminiscent of a Cantor point-set), depending on parameter values. The sections following will show that the subsets of points of zero volume that are visited by Γ depend on both the values of the parameters of **g,** and the number of equilibria at those parameter values. Put differently, parameter values represent different levels of reality.

To make this last assertion clearer, **g** is restricted to $\Re^3$ (where $\Re$ stands for the real line) and rewritten as:

$$\left\{ \begin{array}{c} \dot{\boldsymbol{y}} = \boldsymbol{f}(\boldsymbol{y}; a) \\ \Gamma^+(\boldsymbol{y}_0) = \{\boldsymbol{y} \,\varepsilon\, E / \boldsymbol{y} = \phi_t(\boldsymbol{y}_0),\ t \geq 0\} \\ \Gamma^-(\boldsymbol{y}_0) = \{\boldsymbol{y} \,\varepsilon\, E / \boldsymbol{y} = \phi_t(\boldsymbol{y}_0),\ t \leq 0\} \end{array} \right\}, \tag{1}$$

where the parameter a ε $\Re$, Γ^+ is a positive half trajectory or a stable orbit passing through $\mathbf{y}_0$; Γ^- is a negative half-trajectory or an unstable orbit through $\mathbf{y}_0$, both defined by (1), such that $\Gamma = \Gamma^+ \cup \Gamma^-$, and $\mathbf{y_0}$ is any point in U (.).

To distinguish between conservative and dissipative systems, it must be emphasized that (1) is a dissipative systems characterized by volume contraction. That is, if all orbits that cross U (B) do so in an inward direction, then B is positively invariant and its divergence is:

$$div\ (\boldsymbol{f}) = \Sigma_{i=1}\ \partial f_i\ (.)/\partial\, y_i < 0, \quad i = 1,\ 2,\ 3; \tag{2}$$

that is, div (**f**) is a strictly negative constant.

This implies that all orbits that begin in U (B) at time t will end up in some new image set of B (denoted ϕ_τ (B)) at time t + τ under the transformation **f**. Integrating forward from all initial values in U (B) from t to t + τ yields:

$$\phi_\tau\ (.) = \boldsymbol{y}(t + \tau) = \boldsymbol{y}(t) + \int_t^{t+\tau} \boldsymbol{f}(\boldsymbol{y}(t))/d\tau, \tag{3}$$

where the integral is a vector with 3 components (f_i).

Let V(t) be the volume of U (B) at time t, V(t + τ) be the volume of ϕ_τ (B) at t + τ, and let D_τ be the determinant of the Jacobian matrix β of the transformation ϕ_τ (.), where,

$$D_\tau = det\ \partial\ \phi_\tau\ (\mathbf{y}(t))/\partial(\mathbf{y}(t)) \tag{4}$$

It can then be shown, after some extensive manipulation of which the reader is spared, that:

$$V\ (t\ +\ \tau) = \int\int\int_\beta D_\tau\ dy_1\ dy_2\ dy_3, \tag{5}$$

where β is the Jacobian matrix of **f** evaluated at **y** (t). After differentiating (5), we have:

$$dV(t)/dt = lim_{\tau\to 0}\, dV(t + \tau)/d\tau = \int\int\int_\beta Tr(\beta)\ dy_1\ dy\ dy_3 \tag{6}$$
$$= \int\int\int_\beta div(\mathbf{f})\ dy_1\ dy_2\ dy_3.$$

Since div(**f**) < 0, it follows that dV/dt = div(**f**). V < 0, as V is similar to a Lyapunov function. Integrating, we have:

$$V\ (t)\ =\ m\ e^{\ div(\mathbf{f})\ t},\ where\ m\ is\ a\ positive\ constant. \tag{7}$$

Obviously, volume shrinks to zero, and all orbits reside in B, the attractor. It should also be noted that the "thin" set in $\Re^3$ is not a single point or a closed orbit. As remarked above, subsets of points of zero volume (Γ_s, Γ_u, Γ_d) will appear as the parameter *a* is varied. Additionally, in the social sciences, such as economics and finance, the attractor contains a subset of inherent noise, Γ_n, which cannot be filtered out since it is due to the incompleteness of information sets of traders at the instant of exchange. The observed output of **f** (henceforth, Z_t), as a reflexive dynamical process, can be filtered for white noise and measurement errors, but the noisy subset Γ_n cannot. Obviously, incomplete information leaves room for false signaling or even price manipulation by big traders, which becomes pathological when the attractor becomes strange, as we will explain shortly. For the time being, however, let us say that all is not lost. As alluded to above, *B is a collection of branched and interleaved zero volume subsets that are visited by different orbits depending on parameter values, but the impacts of Γ_n are restricted to specific values of the parameter.* The branched and interleaved attractor may also be written as Ƀ = $\cap_{\tau\geq 0}$ (ϕ_τ (B)). To make this last assertion constructive, we now turn to the quadratic map.

2.2 The H Exponent as a Measure of Complexity

Quadratic maps are well-studied prototypical strange attractors in (0, 1) → (0, 1) that happen to characterize the universal law of growth. *Ex hypothesi*, their thrown-offs should effectively characterize H as well.

Suppose that the future size of a growing entity (y_{n+1}) is a linear function of its actual size (y_n). That is: $y_{n+1} = a\ y_n$, where *a* > 1 is a growth factor. This is obviously not a realistic growth model as nature forbids outcomes such as $y_n \to\infty$ by imposing an inverse relationship between the actual growth factor [*a* (1 –y_n)] and the size of the growing variable (y_n). Substitution gives:

$$y_{n+1} = f\,(y) = a\ (1\text{-}\ y_n)\ y_n\ ,\ where\ a\ \varepsilon\ (0,\ 4),\ y\ \varepsilon\ (0,\ 1) \tag{8}$$

Thus, as y approaches a limiting value (in this case 100 percent or 1.0 on the unit interval), the growth factor falls to zero as shown in (8). That equation is the well-studied logistic parabola, a recursive form of the J-F. Verhult's (1804-1845) equation that has become the work-horse in non-linear analyses in many fields. Denoting «y» and y* as the mean and the equilibrium size of the variable, respectively, we have «y» = 1/2, y* = 0 for *a* ≤ 1, and y* = [(*a* – 1) / a] for *a* > 1. The derivative of (8) is f'(y) = *a* (1 – 2y*) = *a* for y* = 0 or (2 –*a*) for y* ≠ 0 at other fixed-points. Fixed-points are stable if f'(.) = *a* (1-2y) ε [-1, 1); of particular interest is |f'(.) | = 0, which represents a super-stable equilibrium.

Experimental work carried by Los (2000) shows that H varies from ≈ 0.98 to almost zero over the span of *a*. For our purpose, however, the span of *a* can be divided into 3 specific zones:

I- $1 < a < [1 + (6)^{1/2}\ ] \to (\Gamma\text{-}2^0, \Gamma\text{-}2^1, \Gamma\text{-}2^2) \to f\,(.)$ is in a persistent regime (H = 0.92) or monofractality;

II- $[1 + [(6)^{1/2}] < a < 1 + (8.0738)^{1/2}] \to \Gamma\text{-}2^k, \Gamma\text{-}3x2^k$, k = 2, 3, 4,…→ $f\,(.)$ is anti-persistent or a multifractal;

III- $[1 + (8.0738)^{1/2}] < a \leq 4 \to$ is the chaotic region according to Definition 2, $f\,(.)$ is again persistent.

In general, at 1 < *a* ≤ 3, only fixed-point orbits of period 1 exist and are visited, but at exactly *a* = 3, the fixed point becomes marginally stable. At *a* = 3.14 or there about, Γ^+ jumps to Γ^- until *a* = 3.23 where it jumps back to Γ^+ again, producing two equilibria: y* = 0.500, and y* = 0.809….At that point, the orbit travels 0.309 in one direction, but another leave is added in the other direction. At *a* = 3.34, the orbit jumps to the unstable manifold again until *a* = 3.498561 where 4 equilibria result; the orbit must now travel a distance equal to 0.874 – 0.383 = 0.491…. and more leaves are added. Clearly, the size of B has increased and continues on increasing until *a* = 3.84, but with a bust of persistence at *a* = 3.75 due to the appearance of a stable orbit. Between 3 < *a* ≤ 3.569446,

equilibrium points will be visited by orbits of periods 2^k, k = 1, 2, 4, 8, etc. And 3.569446… < a ≤ 4, known as the "chaotic regime" (different from the chaotic region), there exist an infinity of equilibrium points to be visited; in fact, at a = 3.569446…, denoted a_∞, the motion of f (.) is aperiodic, comprising a Cantor point-set of infinitely many values of y that never repeat. And within the chaotic regime, up to the period 3 window (according to Li and Yorke (1975)), there exist an infinite number of a values for which motion is stable and unstable. Within the period-3 window, there are 3 chaotic intervals followed by renewed period doubling, but orbits are of period $3x2^k$, k = 1, 2, 3,…. For example, just before reaching the period-3 window, intermittent period-3 pulses will be observed. Inside the window, there are 6 fixed-points by virtue of the up and down movements of the hills and valleys of the third iterate; 3 are stable and 3 are unstable. But once period-3 cycles appear, there will be cycles of all orders, some will be stable, others will not. Beyond the period-3 window, but up to a = 4, there is SDIC; therefore, motion is chaotic in the sense of Definition 2. Even though orbits are mostly chaotic and unstable in that interval, there are however a few stable orbits depending on values of a. And at a = 4, there is a countable number of periodic cycles, an uncountable number of aperiodic ones, and a dense orbit.

What Los' analysis reveals is that the process is anti-persistent in zone II, and persistent elsewhere. Using the Hausdorff measure, Figure 1 reveals a similar story. The process is anti-persistent from the second bifurcation to the end of period-3 window; that is, over the interval: 3.498561… < a < 3.841499…. In that interval, variations of H with respect to a are reminiscent of a Weierstrass function, and this is precisely the region of multiple equilibria (stable and unstable) and where the process becomes more sensitive to the parameters (SDP). The presence of a greater number of equilibria that must be visited and the fact that the iterates of the map tend to migrate toward the Cantor point-set and other accumulation points, cause compression and stretching , thereby increasing not only the size of B but the level of complexity as well. Whereas in the interval 1 < a < 3.49…., H (or H) is persistent; over the interval 3.84…< a ≤ 4, H is again persistent, albeit Weierstrass-like. Before we attempt to explain this, we need to define *period-doubling*. It is a phenomenon whereby more and more stable fixed-points (Γ^+) lose their stability (Γ^-) and bifurcate to more fixed-points (Γ^+, Γ^-) that are now crowded in the same unit interval; this occurs over the intervals 3.49… < a < 3.56…, and within the period-3 window. From a = 3.56… to a = 3.84…, another phenomenon occurs. It is referred to as *intermittency* whereby a local bifurcation increases the size of the existing attractor, but preserves its locus. The larger attractor may or may not be chaotic depending on the phase space prevailing before the bifurcation. Examples of this are seen at a = 3.63, a = 3.75, a = 3.87, etc.

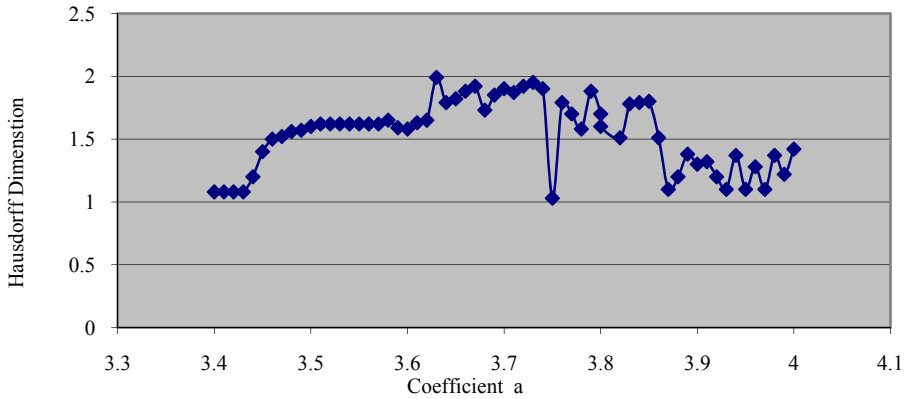

Figure 1. The Hausdorff Dimension vs. the Coefficient a

As shown in Figure 1, the Persistence subset H ε [1, 1.5), the Anti-persistence subset H ε (1.5, 2]. In other words, H is anti-persistent in Zone II and persistent elsewhere. Then:

Assertion 1:Anti-persistence is a consequence of the conjunction of period doubling and intermittency (a. s.).

Assertion 2: As a stochastic process moves from persistence to anti-persistence, every element of the set of Renyi' s (1970) generalized fractal dimensions undergo an increase in size (a. s.).

We will substantiate Assertion 2 in Section 4; in particular, we will show a general increase in the Hausdorff dimensions which measure how the attractor fills up space.

Incidentally, it should be noted, on the one hand, that at $a = 4$, Los (2000) has found H to be 0.58 (or H = 1.42) rather than 0.5 as one would expect. We do not have an explication for that counterintuitive result. It could be due to a number of reasons. For example, due to the fact that chaotic and non-chaotic values of a are interwoven, giving rise to SDIC, to increased SDP, to an infinite number of unstable orbits, or due to the fact that the logistic map is not strictly self-similar. What is more compelling though is that an experiment carried out by Medio (1992) has shown that the addition of a small amount of noise suffices to make all values of computed trajectories in the whole chaotic regime spurious. This then confirms that Γ_n intersects other subsets at a lower level of reality. It also means that in the capital market where the noise floor of the attractor is not empty, the accuracy of computed values in anti-persistence mode as well as statistical predictions thereof are questionable.

The clues thrown-off by the iterative construction of (8) are to be taken seriously, because they are generic. The only difference between (8) and other quadratic maps stems from the differences of interval values. Table 1 below examines the logistic parabola in (8) and two other maps studied by Grassberger (1981). It can be seen that at the point of aperiodicity (in 1-D), the three maps have the same Hausdorff measure (H) (see below and Appendix 1). That is,

$$dim_H(f((y)) = dim_H((f(x)) = dim_H((f(z)) = 0.5388.... \pm 0.002 \quad (9)$$

2.3 The Centrality of the Hausdorff Dimension

In Appendix 1, to which the reader is referred, the Hausdorff dimension is shown to be not only a more efficient measure than either the topological or the box-counting dimensions, but also a more natural measure within the multifractal formalism. To be more explicit: If du (b) exists (see A.1.3), then $B_\alpha = \{b$: the limit du (b) = $\alpha\}$ is the set for which the limit exists and is equal to α, where α is the Lipshitz-Holder mass exponent; then there is a decomposition of B by level sets for which the limit does not exist. Therefore, the dimension spectrum is a function f_u: $\Re \rightarrow \Re_{(0, d)}$, given by $f_u(\alpha) = \dim_H(B_\alpha)$. Then the multifractal analysis of the measure u describes the size of the set B_α through the behavior of f_u. Hence, $\dim_H(B_\alpha)$ is a natural measure characterizing the multifractal properties or quantifying the non-uniformity of the multifractal spectrum.

As regards i) and ii) in Appendix 1, consider a cover $u = \{u_i\}$ for a given set X by open sets. For a $\delta > 0$ and diam $u_i \leq \varepsilon$, then it is shown in Warwick (2012) that $\dim_H(X) = \inf\{\delta: H^\delta(X) = 0\}$. Therefore, $\dim_H$ satisfies both i) and ii).

It follows that $\dim_H(B)$ is the appropriate measure for the set B whether in persistence or an-persistence mode. In addition, it is a central element in the set of Renyi's generalized fractal dimensions to which the next section is devoted.

2.4 The Multifractal Spectrum

The original method of multifractal cascades is known nowadays as the multifractal formalism. Mandelbrot introduced it in response to systematic experimental deviations observed in the Kolmogorov theory of homogenous and isotropic turbulence (Mandelbrot, 1974; Frish, 1995). It has since undergone considerable theoretical developments and practical applications in many disciplines, because it seems well adapted to reveal the hierarchy governing the spatial distributions of singularities of multifractal measures. Naturally, the tendency is to just transfer it to financial series analyses (Lux, 1996; Lobato & Savin, 1998; Calvert & Fisher, 2002; Kesterner & Arneodo, 2003, among others) without however paying heed to the fact that the capital market is a reflexive construct that is neither globally self-similar nor governed by a noise free attractor.

The singularity spectrum of a non-linear input/output process, generating an output Z_t with fractal properties, depends on input conditions. This then suggests that the appropriate process for financial analysis is the Mixed fractional Brownian motion (MfBm) (see, Zili, 2006; Maio, *et al*., 2008; Thale, 2009; Dominique & Rivera, 2011).

Table 1. Three quadratic maps with the same properties over different intervals. Values indexed by ∞ mark the end of Period-Doubling

Function	Mean « »	Equilibrium (*)	Aperiodicity ($_\infty$)	Chaotic Regime
$f(y) = a\, y_n (1 - y_n)$ $y \varepsilon (0, 1)$; $a \varepsilon (0, 4)$	1/2	$(a - 1) / a$	$a_\infty = 3.569446\ldots$	$a_\infty < a \leq 4$
$f(x) = b(1 - 2x^2)$ $x \varepsilon (-1, 1)$; $b \varepsilon (-b, b)$	0	$[(1 + 8b^2) - 1] / 4b$	$b_\infty = 0.837005\ldots$	$b_\infty < b \leq 1$
$f(z) = c\, z(1 - z^2)$ $z \varepsilon (0,1)$; $c \varepsilon (0, 2.59)$	$(1/3)^{1/2}$	$[(c - 1) / c]^{1/2}$	$c_\infty = 2.300228\ldots$	$c_\infty < c \leq 2.5988\ldots$

Definition 3: $Z_t = \sum i^n (r_i X^{Hi})$, *where* $r \varepsilon \Re$, $i \varepsilon n$. *and* $H_i \varepsilon (0,1)$, $\forall i \varepsilon n$.

Z_t is an observed combination of Gaussian processes (X^{Hi}), each with its own H index. X^{Hi} are the unobserved Mandelbrot-van Ness (1968) inputs into Z_t, arriving as "cars" or "trains" in the terminology of Sottinen (2003). Z_t not only captures the properties of the dynamic input/output construct describing the financial market, but its structure allows the analysis of the data segment by segment, depending on their scaling limit of self-similarity. That setting allows the judicious use of both the wavelet multi-resolution analysis and the Mandelbrot Method of multifractal analysis. For, if outputs are only approximately self-similar, they must be decomposed into subsets supporting a Borel probability measure having some sort of symmetry which can reproduce copies of the sets on arbitrarily small scales up to a given precision (For more on this, see Arneodo, *et al*., 1995, 2000). In the next section, the S&P-600 Index is taken as Z_t and the Renyi's dimensions are computed using the Mandelbrot Method.

3. The Data and Method of Computation of Renyi's Dimensions

We use the grand Microsoft Excel Data set of closing prices of the S&P-500 Index, from January 3rd, 1950 to February 28th, 2011, sampled at daily intervals, and expressed as an MfBm of Definition 3. The whole index was divided into 12 segments, but for the present purpose, it was convenient to consider 7 segments which were next de-trended using logarithmic differences and filtered for white noise. That is, 3 segments during which the index was persistent and 4 when the index was anti-persistent; their lengths vary from 2^9 to 2^{11}.

The analysis is done in two stages. In the first, we use the wavelet multi-resolution software of Trusoft International, the Benoit version, to determine the boundaries of the Hurst exponents (H) as well as the Hausdorff dimensions ($D_0 = \dim_H$). In the second stage, D_0 is used as the starting point in the determination of the generalized fractal dimensions and the singularity spectra of each segment.

The Mandelbrot Method (MM) (see Appendix 2) is a simple iterative construction that asymptotically models strange attractors. It consists of an "initiator" (the unit interval) and a "generalized generator" (ρ) with two intervals (e_i), i ε (1, 2). The initiator is first divided into two bins with equal probability (p_i). Next, the exponent q is assigned to the probabilities, while the exponent τ is assigned to the support intervals.

Quadratic maps have the same structure, but different intervals. Hence, the sizes of generators vary with interval sizes. Experimentally, Schroeder (2009, 276) has found an interval size $e_1 = 0.4000$ to be a good approximation of e_i for the logistic map. But using (A.2.1'') in Appendix 2, $e_1 = 0.408903\ldots$ which is equivalent to a generalized generator of $\rho = 2.445564\ldots$ instead of the experimental value of 2.5 approximated by Schroeder; again this is due to the fact that the maps are not exactly self-similar. Since the appropriate map of a given process may not be known in advance, one should appeal to (A.2.1'') to yield the sizes of the generator and intervals from the Hausdorff dimension obtained from the wavelet multi-resolution analysis. Once e_1 is known, all the Renyi' generalized fractal dimensions, except of course for D_1, can be computed using a handheld calculator. Next, from the Legendre Transform: $\alpha(q) = -d\tau(q)/dq$; $df(\alpha)/d\alpha = q$; $f(\alpha) = q\, d\tau/dq - \tau(q)$, the multifractal spectrum can be constructed. Thus, the generality of D_0 in this approach cannot be over-emphasized; it is valid for any set B as shown in (9).

4. The Results

The results of the first stage are given in Table 2. It shows that the index fluctuated between persistence (1961-72, 1983-87, and 1998-02) and anti-persistence (1972-83 and from 2003-11), but at no point the so-called "efficient market" value (H = 0.5) was observed

Table 3 presents the results of the second stage. The Renyi's generalized dimensions were calculated according to (A.2.2) and (A.2.3) in Appendix 2. Recalling that the multifractal spectrum $f(\alpha)$ describes the dimension of a subset with a Lipshitz-Holder mass exponent α. But both $f(\alpha)$ and $\tau(q)$ give the same description of the multifractal. Hence the information is given in terms of D_q and the 3 α-values which delimitate the size of the spectrum. Table 3 reports the generalized dimensions in successive time intervals, drawn from the affine profile of the index. Later on, we will comment on the meaning of these dimensions and on how they may be converted into 3-D.

The arrangement of Table 4 is different. The first 4 columns represent the state of anti-persistence. As shown, for the higher value of the Hausdorff dimensions, the spans of the singularity spectra are also larger, characterizing the state of anti-persistence. In the last 3 columns, Hausdorff dimensions are lower, and the spans are smaller, depicting the state of persistence. It can then be concluded that if: $\dim_{Hi} > \dim_{Hj}$, $(\alpha_{\max i} - \alpha_{\min i}) > (\alpha_{\max j} - \alpha_{\min j})$, then j is more persistent than i. In other words, the lower is $\dim_H$, the smaller is the convex set of $HG_{f\alpha}$, where HG_f is the hypograph of $f(\alpha)$, defined as:

$$HG_f = \{(\alpha, f)\ \varepsilon\ \Re^2/_\alpha \leq f(\alpha)\} \tag{10}$$

As the index jumps from persistence (H > 1/2) to anti-persistence (H < 1/2), both spans and maxima of multifractal spectra, which are equal to the Hausdorff dimensions, increase in accordance with Assertion 2.

Table 2. Properties of Locally self-similar segments of the S&P-500 Index, sampled daily from January 1950 to February 2011

Period	Number of observations	Hurst Exponent H	Hausdorff Dimension H
1961-72	2^{11}	0.5220…± 0.00321	1.4780
1972-80	2^{11}	0.2209…± 0.0359	1.7791
1983-87	2^{10}	0.5590…± 0.0501	1.4410
1998-02	2^{10}	0.6100…± 0.0612	1.3900
2003-07	2^{10}	0.1101…± 0.0310	1.8899
2007-08	2^{9}	0.2811…± 0.0326	1.7189
2009-11	2^{9}	0.1430…± 0.0339	1.8570

4.1 More on the Dimensions

As shown in Table 3, at q = 0, the Hausdorff dimension, identified as $D_0 = \dim_H$ is recovered. As discussed in Appendix 1, D_0 is robust and natural enough in the singularity spectrum to describe many different aspects of the attractor.

Some authors claim that D_0 describes the geometry of the fractal set while others prefer to describe it as the dimension of the measure (u) which weighs all portions of the attractor equally. And there are those who describe it as a space filling measure. However defined, it is important to stress that it is a universal element in all singularity spectra of strange attractors.

The subset $D_{(q<0)}$ (or the negative Renyi's dimensions) measures the degree of emptiness of empty subsets. They are used mainly to analyze super samples in turbulence and in diffusion-limited aggregation (DLA); the latter addresses the motion of molecules in biological growth patterns which are beyond the scope of this study. The other subset $D_{(q>0)}$ describes the densest part of the attractor. To wit:

D1 is a function of the entropy of the probabilities (p_i), and an element of Claude Shannon's formula. The entropy and D_1 describes the loss of information as a non-linear dynamic system, which may be chaotic, evolves in time. From the function f(α), df(α)/dα =1, hence $D_1 = f(\alpha_1)$ (= α_1) lies on the tangent of the f(α) curve with slope = 1 through the origin. It may also describe the frequency with which orbits visit different part of the attractor.

Table 3. Renyi's Generalized Fractal Dimensions of dated locally self-similar segments of the S&P-500 Index, 1950 -2011

	1961-72		1972-83		1983-87		1998-02	
q	α	D_q	α	D_q	α	D_q	α	D_q
0	α_0 = 1.594771	1.478000	α_0 = 1.922390	1.779100	α_0 = 1.556798	1.441000	α_0 = 1.501700	1.3900
1		1.419212		1.708338		1.383684		1.334715
2		1.368818		1.646771		1.646771		1.287317
3		1.326549		1.596797		1.293341		1.247567
…		…		…		…		…
∞	α_{min} = 1.064798	1.064798	α_{min} = 1.282361	1.282361	α_{min} = 1.038142	1.038142	α_{min} = 1.001400	1.001400
-1		1.543381		1.857803		1.504744		1.451489
-2		1.611911		1.940293		1.571558		1.515938
-3		1.678386		2.020311		1.636369		1.578455
…		…		…		…		…
-∞	α_{max} = 2.128745	2.128745	α_{max} = 2.562419	2.562419	α_{max} = 2.075454	2.075454	α_{max} = 2.00200	2.00200

Table 3. Continued

	2003-07		2007-08		2009-11	
q	α	D_q	α	D_q	α	D_q
0	$\alpha_0 = 2.041360$	1.888900	$\alpha_0 = 1.856594$	1.718900	$\alpha_0 = 2.005709$	1.857000
1		1.814900		1.650632		1.783247
2		1.750450		1.592015		1.719921
3		1.696224		1.542697		1.666641
…		…		…		…
∞	$\alpha_{min} = 1.360630$	1.360630	$\alpha_{min} = 1.237478$	1.237478	$\alpha_{min} = 1.336900$	1.336900
-1		1.971447		1.793009		1.937063
-2		2.060801		1.874276		2.024859
-3		2.146308		1.952043		2.108875
…		…		…		…
-∞	$\alpha_{max} = 2.722090$	2.722090	$\alpha_{max} = 2.475710$	2.475714	$\alpha_{max} = 2.674614$	2.674714

Table 4. The impact of persistence on the singularity spectrum of the S&P-500 Index, 1950-2011

Period	2003-07	2009-11	1972-80	2007-08	1961-72	1983-87	1998-02
$\dim_H$	1.8899…	1.8570…	1.7791…	1.7180…	1.4780…	1.4410…	1.3900…
Spectrum Span	1.361460	1.337714	1.280058	1.238232	1.063947	1.037312	1.000600
	ANTI-PERSISTENCE				PERSISTENCE		

D_2 is determined by the correlation function of the fractal set; that is, the probability of finding a given member of the set within a distance λ of another member. It is also viewed as a probability measure of the frequency with which orbits visit different part of the attractor. That measure was developed by Grassberger and Procaccia (1983) in 3-D for the purpose of reconstructing unknown attractors. It distinguishes between deterministic chaos and pure random- ness in a set if the number of points is sufficiently large, evenly distributed, and if the generating mechanism is not too complex and free from noise (De Coster & Mitchell, 1991). The main difference between the value of D_2 in Table3 and the Grassberger-Procaccia measure is that in the latter one must guess the dimension of the unknown attractor and seek convergence on some embedding dimension. This then introduces an additional variable in the process. For example, Medio (1992, 209- 210) uses that procedure on slightly modified logistic map and arrives at a value of approximately 2.15. If we were to compare that value with the D_2 found in Table 3, when the Hausdorff dimension was 1.3900…, we would get $D_2 = 1+ 1.287319 = 2.28$…. To take another example, consider the finding of Peters (1991). He used the Grassberger and Procaccia procedure to compute D_2 of the S&P-500 Index, sampled monthly from January 1980 to July 1989, and found a value of 2.33. In Table 3, our value of D_2 from 1983-87 is $D_2 = 1 + 1.334551= 2.334551$…. In fact, 3 seem to be a limiting value for strange attractors (see Section 2.1). Experimental findings consistently indicate to that effect that chaotic attractors have non-integer dimensions $2 < D < 3$, regardless of the size of the phase space (for more on this, see Invernizzi and Medio, 1991; Medio, 1992, 130-133).

Finally, D_∞ measures the densest part of the attractor, while $D_{-\infty}$ describes the sparsest part. Thus, the set of generalized dimensions is very useful for quantifying the non-uniformity of the fractal set and for characterizing its multifractal properties at the same time. However, the fact that some of our values are carried out to six decimal places is to recall their asymptotic characters and not a claim to precision. In general, the goal of dimension estimation is a qualitative assessment to distinguish chaos from random determinism. Hence, a robust and simple estimate of dimensions is more useful than a precise estimate.

5. Conclusions

The MfBm process of Definition 3 reveals that the S&P-500 Index exhibits short and long-term dependence. While the thrown-offs of quadratic maps indicate that anti-persistence results from intermittence and the period-doubling scenarios. As a consequence, the sizes of all the elements of the set of Renyi's generalized fractal dimensions, which through the Legendre Transform yield the singularity spectrum of a fractal set, undergo an increase. The compelling conclusion is that anti-persistence increases the hypograph of the singularity spectrum of a multifractal. This is demonstrated in Tables 3 and 4.

The analysis also reveals that the non empty noise subset of the strange attractor of the S&P-500 Index is operational over the whole range of the chaotic regime, which includes the anti-persistence regime; over that large window, the accuracy of computed values becomes suspect. This would mean that the observed price level

can never accurately reflect fundamentals. Spurious prices would create spurious excess demands that the market would attempt to dissipate, thereby creating more imbalances until participants realize the spuriousness of observed prices. Knowledge of this which may come at any moment, however, elicits a correction in input arrivals which more often than not is translated in withdrawals of resources from the market. Therefore, market crashes are belated corrections occurring in anti-persistence mode.

Effectively, a significant fall in H occurred in mid-1972. That fall must be seen in retrospect as a precursory sign of the market crash of 1972-73. The reason seems to have been a change in investors' behavior following the abrogation of the Bretton Woods Agreements and the oil embargo of 1973. During the period of 1972-80, the index remained in flicker noise territory until the crash of 1981-82. It did recover by mid-1997 because the IT bubble was ongoing, but imbalances continued to accumulate until the crash came in 2000-01 and beyond. In June 2002, the index became even more anti-persistent and remained there until the 2007-08 crash. Table 4 shows that the index had not emerged from anti-persistence by February 2011, which is the last period for which we have data. These developments show that almost surely, anti-persistence is a consequence of investors' behavior as their expectations collapse (see Table 2).

As indicated at the outset, theorists have found that the computed values of the H exponent were varying with series lengths, with sampling intervals, and over time. Figure 1 above explains these variations.

The attempt to characterize anti-persistence has thrown off a number of additional conclusions. First, the noisy subset of the attractor is due to incomplete information such as uncertainty, false signaling or price manipulations (think of the rate of interest). As such, the noisy subset seems to reflect a double half-Heisenberg's dilemma. Theoreticians would like to know "true" prices which are not knowable except in perfectly competitive settings, while practitioners would like to eliminate the noisy subset which is not doable. One way to make this dilemma mitigable is an increased surveillance of the Hausdorff dimensions of markets in non perfect competitive settings. That is, the minute $\dim_H > 1.5$, steps should be taken to restore participants' confidence in the market.

Man-made constructs are not globally self-similar. The impact of noise is pervasive in anti-persistence mode. The second thrown-off indicates that the best that can be done to mitigate such constraints is a greater use of fBm's conjointly with the wavelet multi-resolution, while emphasizing the qualitative aspects of measures from the multifractal formalism.

Finally, the application of the Mandelbrot Method makes it simpler to estimate the correlation dimension of a fractal set than does the Grassberger-Procaccia procedure (see Section 4.1).

References

Alvarez-Ramirez, J., Alvarez, J., Rodriguez, E., & Fernandez, A. (2008). Time-varying Hurst exponent for US stock markets. *Physica A*, 1959- 1969.

Arneodo, A., Bacry, E., & Muzy, J. F. (1995). The thermodynamics of fractals revisited with wavelets. *Physica A*, *213*, 232-275. http://dx.doi.org/10.1016/0378-4371(94)00163-N

Arneodo, A., De Coster, N., & Roux, S. G. (2000). A wavelet-based method for multifractal image analysis. *European Physical Journal B, 15*, 567-600.

Calvert, Laurent, E., & Fisher, Adlai, J. (2002). Multifractal in asset returns: theory and evidence. *Review of Economics and Statistics, 84*, 381-406. http://dx.doi.org/10.1162/003465302320259420

Cutland, N. J., Kopp, P. E., & Willinger, W. (1993). Stock price returns and the Joseph effect. A fractal version of the Black-Scholes model. *Progress in Probability*, *36*, 327-351.

De Coster, G. P., & Mitchell, D. (1991). The efficiency of the correlation dimension technique in detecting determinism in small samples. *Journal of Statistical Computation and Simulation*, *39*, 221-229. http://dx.doi.org/10.1080/00949659108811357

Dominique, C-R., & Rivera, S. L. (2011). Mixed fractional Brownian motion, short and long-term dependence and economic conditions: The case of the S&P-500 Index. *International Business and Management*, *3*, 1-6.

Eckmann, J. P., & Ruelle, D. (1985). Ergotic theory of chaos and strange attractors. *Review of Modern Physics*, *57*, 617-656. http://dx.doi.org/10.1103/RevModPhys.57.617

Frish, U. (1995). *Turbulence*. Cambridge: Cambridge University Press.

Grassberger, P. (1981). On the Hausdorff dimension of fractal attractors. *Journal of Statistical Physics*, *26*, 173-179. http://dx.doi.org/10.1007/BF01106792

Grassberger, P., & Procaccia, I. (1983). Characterization of strange attractors. *Physical Review Letters*, *50*, 346-349. http://dx.doi.org/10.1103/PhysRevLett.50.346

Greene, M. T., & Fielitz, B. D. (1977). Long-term dependence in common stock returns. *Journal of Financial Economics*, *4*, 339-349. http://dx.doi.org/10.1016/0304-405X(77)90006-X

Hurst, E., *et al*. (1951). Long-term storage: An Engineering study. *Transactions of the American Society of Civil Engineers*, *116*, 770-790.

Invernizzi, S., & Medio, A. (1991). On lags and chaos in economic dynamic models. *Journal of Mathematical Economics*, *20*, 521-550. http://dx.doi.org/10.1016/0304-4068(91)90025-O

Kaplan, L. M., & Jay Kuo, C. C. (1993). Fractal estimation from noisy data via discrete fractional Gaussian noise and the Haar Basis. *IEEE Transactions*, *41*, 3554-3562. http://dx.doi.org/10.1109/78.258096

Kesterner, P., & Arneodo, A. (2003). Three-dimensional wavelet-based multifractal method: The need for revisiting the multifractal description of turbulence dissipation data. *Physical Review Letters*, *91*, 194501. http://dx.doi.org/10.1103/PhysRevLett.91.194501

Li, Y. L., & Yorke, A. (1975). Period three implies chaos. *American Mathematical Monthly*, *82*, 985-992. http://dx.doi.org/10.2307/2318254

Lobato, I. N., & Savin, N. E. (1998). Real and spurious long-memory properties of stock market data. *Journal of Business and Economic Statistics*, *16*, 261-268. http://dx.doi.org/10.2307/1392503

Los, Cornelis, A. (2000). Visualization of chaos for finance majors. *Working Paper* 00-7, School of Economics, Adelaide University.

Lux, T. (1996). Long-term stochastic dependence in financial prices: evidence from the German stock market. *Applied Economics Letters*, *3*, 701-706. http://dx.doi.org/10.1080/135048596355691

Maio, Y., Ren, W., & Ren, Z. (2008). On the fractional mixed fractional Brownian motion. *Applied Mathematical Science*, *35*, 1729-1738.

Mandelbrot, B. (1974). Intermittent turbulence in self-similar cascades: Divergence of high moments and dimension of the carrier. *Journal of Fluid Mechanics*, *62*, 331-358. http://dx.doi.org/10.1017/S0022112074000711

Mandelbrot, B., & van Ness, J., W. (1968). Fractional Brownian motions, fractional noises and applications. *SIAM Review*, *10*, 422-437. http://dx.doi.org/10.1137/1010093

Medio, A. (1992). *Chaotic dynamics: Theory and applications to economics*. Cambridge, UK: Cambridge University Press.

Peters, E. (1991). A chaotic attractor for the S&P-500. *Financial Analyst Journal*, March/April.

Renyi, A. (1970). *Probability Theory*. Amsterdam: North-Holland.

Schroeder, M. (2009). *Fractals, Chaos, Power Laws*. New York: Dover Pub., Inc.

Sottinen, T. (2003). Fractional Brownian motion in finance and queuing. (Doctoral dissertation). University of Helsinki, Finland.

Thale, C. (2009). Further remarks on mixed fractional Brownian motion. *Applied Mathematical Sciences*, *3*, 1-17.

Warwick. ac.uk. (2012). Lectures on fractals and dimension theory. Homepages.warwick.ac.uk/mas dbl/dimension-total.pdf.

Zili, M. (2006). On the mixed fractional Brownian motion. *Journal of Applied Mathematics and Stochastic Analyses*, *2006*, 1-9. http://dx.doi.org/10.1155/JAMSA/2006/32435

Appendix 1

According to Warwick's ac.uk (2012) lecture on Fractals and Dimension Theory, the Hausdorff dimension is a description of the geometry of a fractal set. If B is a fractal set whose dimension is sought, then let C (e, C) = [c_1, c_2,, …,c_u] be a finite covering of B into sets whose diameters are less than e. Then $B \subset U_i\ c_i$ and the dimension of its set satisfy some $\delta_I = \delta\ (c_i)$. If the function:

$$f\,(B, D, e) = inf\, c_{(B,\,e)} \sum_i \delta_i^D, \tag{A.1.1}$$

where the infimum (over all coverings satisfying $\delta_I < e$) defines a measure for the set B. Then f (B, D, e) decreases monotonically with D. Therefore, there is a unique transition point H that satisfies the Hausdorff dimension. That is:

$$f(B, D, e) = \lim\sup_{e \to 0} f(B, D, e) = \infty \text{ for } D < D_H, \text{ and } 0 \text{ for } D > D_H \quad \text{(A.1.2)}$$

so that $D_H = \inf [D: f(B, D, e)] = 0$ (D_H is henceforth denoted, ($\dim_H$).

For a greater ease of exposition, one might wish to define a probability u on B and consider upper and lower dimensions of u as measurable functions du and du^-, where

$$du(b) = \lim\sup_{e \to 0} \log [\text{ball}(b, e)] / \log e \geq d, \ \forall b \in B, \text{ then } \dim_H(u) \geq d; \text{ and} \quad \text{(A.1.3)}$$

$$du^-(b) = \lim\inf_{e \to 0} \log u [\text{ball}(b, e)] / \log e \leq d, \ \forall b \in B, \text{ then } \dim_H(u) \leq d,$$

where ball (b, e) is a ball of radius e > 0 about b.

Moreover, if a closed bounded set $B \in \Re^n$ is a manifold, the value of its dimension must satisfy the Warwick criteria. That is, its dimension must be:

i) either an integer or a non-integer; and

ii) points and countable unions of points of zero volume must have zero dimension.

It can then be seen that the topological dimension ($\dim_T$), for example, fails on both criteria since it is always an integer, giving 0 for the Cantor set, which is not true. By a similar argument, the Box-counting measure fails on ii), whereas $\dim_H$ (B) satisfies both i) and ii), and $\dim_H (B) \leq \dim_{Box} (B)$.

Appendix 2

The unit interval, the initiator, is divided into two bins of equal probabilities, p_i (i = 1, 2) with exponent q. The generator ρ has intervals e_i to which the exponent τ is assigned. Then the partition function can be written as:

$$\sum_I p_i^q e_i^\tau = 1, \quad i = 1, 2 \quad \text{(A.2.1)}$$

Positing $e_1 = (\rho^{-1})$, $e_2 = (\rho^{-1})^2$, and $\tau(q) = (1 - q) D_q$, where $D_q = \dim_H (.)$ at a given q (Schroeder, 2009; Dominique & Rivera, 2011). It can then be shown that:

$$\dim_H (.) = D_0 = \log [(5)^{1/2} - 1] / \log e_1 \quad \text{(A.2.1')}$$

and

$$e_1 = \log^{-1} [(5)^{1/2} - 1 / D_0] \quad \text{(A.2.1'')}$$

The Renyi's (1970) generalized dimensions of order q are given by:

$$\tau / (1 - q) = D_q = \log_{\lim e1 \to 0} \{[(1 + 4 (2)^q)^{1/2} - 1]\} / (1 - q) \log e_1, \text{ for } q \neq 1 \quad \text{(A.2.2)}$$

For q = 1, D_∞ and $D_{-\infty}$, we have:

$$D_1 = 2 \log 2 / \sum_1^2 \log (1/e_i) \quad \text{(A.2.3)}$$

$$D_{\infty \lim q \to \infty, e1 \to 0} = (- 1/ \log_2 e_1)$$

$$D_{-\infty \lim q \to -\infty, e2 \to 0} = (- 1/ \log_2 e_2)$$